



Published in final edited form as:

J Vitreoretin Dis. 2018 ; 2(3): 146–154. doi:10.1177/2474126418771805.

Imaging the Deep Choroidal Vasculature Using Spectral Domain and Swept Source Optical Coherence Tomography Angiography

J. Daniel Diaz, MD¹, Jay C. Wang, MD¹, Patrick Oellers, MD¹, Inês Lains, MD¹, Lucia Sobrin, MD, MPH¹, Deeba Husain, MD¹, Joan W. Miller, MD¹, Demetrios G. Vavvas, MD, PhD¹, and John B. Miller, MD¹

¹Retina Service, Massachusetts Eye and Ear, Department of Ophthalmology, Harvard Medical School, Boston, MA, USA

Abstract

Purpose—To evaluate the deeper choroidal vasculature in eyes with various ocular disorders using spectral domain (SD) optical coherence tomography angiography (OCTA) and swept source (SS) OCTA.

Methods—Patients underwent OCTA imaging with either SD-OCTA (Zeiss Cirrus Angioplex or Optovue AngioVue) or SS-OCTA (Topcon Triton). Retinal pigment epithelium (RPE) integrity, structural visualization of deep choroidal vessels on en face imaging, and OCTA of deep choroidal blood flow signal were analyzed. Choroidal blood flow was deemed present if deeper choroidal vessels appeared bright after appropriate segmentation.

Results—Structural visualization of choroidal vessels was feasible in all eyes by en face imaging. In both SD-OCTA and SS-OCTA, choroidal blood flow signal was present in all eyes with overlying RPE atrophy (100% of eyes with RPE atrophy, 28.6% of all imaged eyes, $P < .001$).

Conclusions—While choroidal vessels can be visualized anatomically in all eyes by en face imaging, choroidal blood flow detection in deep choroidal vessel is largely restricted to areas with overlying RPE atrophy. Intact RPE acts as a barrier for reliable detection of choroidal flow using current OCTA technology, inhibiting evaluation of flow in deeper choroidal vessels in most eyes.

Keywords

optical coherence tomography angiography; retinal pigment epithelium; choroid

Reprints and permission: sagepub.com/journalsPermissions.nav

Corresponding Author: John B. Miller, MD, Retina Service, Massachusetts Eye and Ear Infirmary, Department of Ophthalmology, Harvard Medical School, 243 Charles St, Boston, MA 02114, USA. john_miller@meei.harvard.edu. J. Daniel Diaz and Jay C. Wang are equal contributors.

Abstract presented at the American Academy of Ophthalmology Annual Meeting, 2017.

Ethical Approval

This study was approved by the institutional review board of Massachusetts Eye and Ear. All procedures adhered to the tenets of the Declaration of Helsinki and HIPAA (Health Insurance Portability and Accountability Act) regulations.

Statement of Informed Consent

Informed consent was obtained when required.

Declaration of Conflicting Interests

The author(s) declared no potential conflicts of interest with respect to the research, authorship, and/or publication of this article.

Introduction

The technology for imaging the choroid using optical coherence tomography (OCT) has evolved over recent years. Early spectral domain (SD) OCT, which utilizes wavelengths near 840 nm suffered from sensitivity roll-off at greater imaging depths. To address this limitation, enhanced depth imaging OCT was developed and allows for better visualization of the choroid by altering the depth of peak sensitivity within SD-OCT. Swept source (SS) OCT utilizes a longer wavelength at 1050 nm which enables deeper penetration and higher spatial resolution imaging of choroidal structures. However, while these technologies have improved structural imaging of the choroid, they do not have the capability to image blood flow.

The recent development of OCT angiography (OCTA) has allowed for the visualization of retinal and choroidal microvasculature by detecting the motion of erythrocytes within blood vessels in successive OCT images over time.¹ Thus far, OCTA has been widely used to study the retinal vasculature in a variety of retinal pathology. However, the choroidal vasculature has not been extensively investigated with OCTA. In fact, reports show that signal attenuation from light scattering, absorption from the retinal pigment epithelium (RPE), and/or from the underlying dense choriocapillaris may limit ability to image the choroidal vasculature.²

In the presence of retinal pigment epithelial atrophy, imaging and detection of blood flow within choroidal vessels may be more feasible with OCTA due to decreased attenuation of signal or scattering of light.³ This has previously only been examined in small case series and only on a single OCTA imaging platform.³ In this study, we sought to evaluate the ability of 3 OCTA imaging platforms, encompassing both SD-OCTA and SS-OCTA, to visualize and detect choroidal blood flow in the deep choroidal vasculature.

Methods

This study was approved by the institutional review board of Massachusetts Eye and Ear (MEE). All procedures adhered to the tenets of the Declaration of Helsinki and Health Insurance Portability and Accountability Act regulations. Informed consent was obtained when required.

This retrospective study identified consecutive patients who underwent OCTA imaging at the MEE as part of their clinical evaluation, including SD-OCTA with the Cirrus HD-OCT Angioplex (Carl Zeiss AG, Oberkochen, Germany), RTvue XR Avanti AngioVue (Optovue, Fremont, California), or SS-OCTA with the DRI OCT-1 Triton (Topcon Europe Medical BV, Capelle aan den IJssel, the Netherlands) from March 31, 2016, to February 1, 2017.

A comparison of the various OCTA systems utilized is shown in Table 1. The Cirrus HD-OCT Angioplex system was the first OCTA-capable Food and Drug administration (FDA) approved device. It utilizes an 840 nm wavelength superluminescent diode light source, obtaining 68 000 A-scans/second. Angioplex utilizes a proprietary algorithm termed optical microangiography, which analyzes phase and intensity information gathered by the scans to

detect differences and visualize the microvasculature. The software allows for segmentation of the choroidal vasculature.

The AngioVue system, which is also FDA approved, utilizes a wavelength of 840 nm and obtains 70 000 A-scans/second with motion correction technology. Optical coherence tomography angiography images are created utilizing a split-spectrum amplitude-decorrelation angiography algorithm. AngioVue software only allows for automatic segmentation of the choriocapillaris. Manual segmentation is needed to assess the deeper choroidal vascular layers.

The Triton DRI OCT-1 system is the first commercially available SS-OCTA device. It has not obtained FDA approval and is used as an investigational device within the United States. All patients who underwent imaging with this system have provided informed consent. The Triton DRI OCT-1 differs from the available SD-OCTA machines, in that it utilizes a longer wavelength scanning light source (1050nm) along with a higher scan speed at 100 000 A-scans/seconds. Topcon's angiographic algorithm is termed OCTA ratio analysis. Choroidal vasculature is not automatically segmented by the software.

Thereafter, basic clinical information was collected and reviewed, including age, gender, diagnosis, and imaging from ancillary studies, such as fundus photography and OCT. B-scan, en face structural OCT and OCTA images (3×3 mm and 6×6 mm) were analyzed for integrity of the RPE and the presence or absence of choroidal flow signal from the choroidal vasculature by 3 investigators (J.D.D., J.W., P.O.) using the built-in review software of Angioplex, AngioVue, and Triton. Note that within each associated software, depth ranges are defaulted to show superficial capillary plexus, deep capillary plexus, outer retina, and choriocapillaris layer. The Angioplex software also segments the deeper choroid automatically. All imaging software allows for manual adjustments. Choroidal segmentation boundaries were selected on the OCTA instruments manually. The choroid was defined as the area between the outer RPE and the inner sclera. Because OCTA is limited in its resolution to image individual vessels in the choriocapillaris, segmentation lines were adjusted to preferentially attempt to visualize the deeper and larger choroidal vessels in Sattler and Haller layers. When a particular case was unclear, all physicians independently reviewed the record. After each physician formed an opinion on the case, the case was discussed to determine its final disposition. Choroidal blood flow was deemed present if deeper choroidal vessels appeared bright after appropriate segmentation on en face OCTA imaging.

The study population demographics were summarized with traditional descriptive measures (ie, means and standard deviations for continuous variables and percentages for binomial/categorical variables). For statistical analysis, given the inclusion of both eyes of the same subject, we used multilevel mixed effect linear models. By definition, these models are appropriate for research designs in which data for participants are organized at more than 1 level (ie, nested data).⁴ All analyzes were performed using Stata, version 14.1 (StataCorp LP, College Station, Texas) and *P* values $<.05$ were considered statistically significant.

Results

Three-hundred ninety-five eyes of 275 patients were included in the study (144 eyes of 91 patients on Zeiss Angioplex, 154 eyes of 77 patients on Optovue AngioVue, and 97 eyes of 54 patients on Topcon Triton). Patient demographic data across the various imaging systems are shown in Table 2.

Table 3 represents a summary of diagnoses and whether choroidal blood flow was visualized. Across all imaging systems, choroidal blood flow was detected in 113 eyes (28.6%). All these eyes had evidence of overlying atrophy of the RPE confirmed by B-scan OCT images ($P < .001$). In these cases, choroidal vessels appeared bright when segmentation lines were adjusted to the deeper choroidal layers. The degree of retinal pigment epithelial atrophy varied across retinal conditions. Structural en face OCT adequately visualized the anatomy of the vascular architecture of large choroidal vessels in all eyes. Large choroidal vessel areas appear dark in en face images, whereas the surrounding choroidal stroma appears bright. In eyes without RPE atrophy, large choroidal vessels likewise appeared dark on OCTA images segmented for the choroid without detection of blood flow. Manual segmentation was attempted in all eyes to improve detection of choroidal vessel blood flow and structural en face visualization.

Optical coherence tomography angiography and en face imaging of choroidal vessels in a normal eye without RPE atrophy using the AngioVue system is shown in Figure 1. Choroidal blood flow was detected in only 23.4% ($n = 36$) of eyes. One hundred percent of these eyes had evidence of RPE atrophy, and choroidal flow was only specifically detected in areas underneath the RPE atrophy (Figure 2).

Similarly, en face OCT images obtained with the Angioplex system allowed for structural visualization of choroidal vessels in all eyes, but choroidal blood flow was detected in 36.8% ($n = 53$) of eyes. Retinal pigment epithelium atrophy was noted in 100% of eyes in which choroidal blood flow was detected. An example of successful detection of choroidal blood flow in an eye with late stage nonexudative age-related macular degeneration is shown in Figure 3.

The SS-DRI OCT-1 Triton system also allowed visualization of choroidal vessels using en face imaging in all eyes. However, this technology also detected choroidal blood flow only in eyes with evidence of RPE atrophy when appropriately segmenting the choroid. An example for this is shown in Figure 4, demonstrating peripapillary choroidal blood flow in an eye with significant peripapillary RPE atrophy.

Scleral projection artifact of the choroidal vasculature was also observed in areas of reduced choroidal thickness in 2 patients with high myopia on both SD-OCTA and SS-OCTA. An example of this artifact is demonstrated in Figure 5.

Conclusion

Consistently across all tested OCTA devices utilizing SD or SS-OCTA technology, choroidal blood flow in deeper choroidal blood vessels was visualized in eyes when there was

evidence of overlying RPE atrophy. In normal eyes and eyes with other retinal pathology, but without evidence of RPE atrophy, choroidal vessels typically appeared dark on OCTA, whereas en face images reliably visualized the anatomical outlines of the choroidal vessels in all eyes, with or without RPE atrophy. Additional adjustment of segmentation lines in order to attempt to best observe flow in deeper choroidal vessels also did not improve visualization of deeper choroidal blood flow. This clearly suggests that visualization of blood flow in deeper choroidal vessels with appropriate segmentation of the choroid is restricted to eyes with evidence of RPE atrophy.

In general, blood flow detected by OCTA is derived from a decorrelation signal from 2 scans taken in rapid succession, with the only difference between the scans being the movement of erythrocytes (following correction for motion, etc).⁵ This signal is displayed as bright on OCTA images per general convention and, at high resolution, can provide detailed 3 dimensional imaging of the retinal vasculature. Despite its potential clinical and investigational value, many investigators feel that OCTA is prone to a wide array of imaging artifacts, including segmentation errors, projection artifacts, motion artifacts, and signal attenuation from overlying hyperreflective material, which can make meaningful interpretation of OCTA images challenging.^{1,6} Thus far, OCTA has been most widely used to image retinal vascular networks; however, imaging of the deeper layers of the choroid has proven more challenging.

Imaging of the choriocapillaris is currently limited by the resolution of the images, which may not be sufficient to visualize the fine individual blood vessels.⁷ Though the images appear grainy, large areas of decreased signal or “flow voids” can be observed in certain conditions that cause loss of the choriocapillaris, such as geographic atrophy and inflammatory chorioretinopathies such as in white dot syndromes.⁸⁻¹⁰ Imaging of the deeper choroidal vessels, however, has not been a major focus of OCTA research thus far.

Using conventional OCTA, choroidal vessels appear dark without any detectable flow. A small case series did demonstrate bright-appearing choroidal vessels in areas of RPE atrophy using the RTvue XR Avanti AngioVue system.³ Furthermore, Kim et al, utilizing phase-variance OCT, visualized choroidal vessels in areas of geographic atrophy, but not from adjacent areas without evidence of RPE atrophy.¹¹ In this study, we confirm that in normal eyes, regardless of the OCTA platform that is used, choroidal flow of large vessels is consistently detected only underneath areas of RPE atrophy. Swept source OCT has been shown to provide improved structural choroidal imaging,¹² but SS-OCTA did not promote improved visualization of choroidal blood flow compared to SD-OCTA.

To our knowledge, there exist 2 major theories to explain why choroidal blood vessels appear dark on OCTA imaging. One postulates that choroidal blood flow velocity is too fast causing fringe-washout phenomenon but that has to be reconciled with the ability to image high-velocity retinal arteries. The other theory states that the OCT signal strength in the choroid is too weak (low signal to noise ratio) with blood flow detection ability below threshold.^{1,11} Our data support the theory that the RPE inhibits detection of the weak signal beneath it in normal eyes using OCTA. We believe that the absence of flow in choroidal vessels on OCTA is caused by reflection/scattering or absorption of light from the RPE,

reducing the amplitude of signal penetrating the RPE. Furthermore, light that reaches the choroidal vessels must pass back through the RPE to be detected, and much of it may be reflected back toward the chorioscleral interface. This may explain why SS imaging, even utilizing a longer wavelength, still does not allow for increased flow visualization of deeper choroidal vasculature compared to SD imaging. The fact that choroidal blood flow can be detected in areas with RPE atrophy suggests that the velocity of blood flow in these vessels is not likely the main barrier for flow detection.

Interestingly, moving the segmentation lines from the choroid to the sclera allowed for visualization of choroidal flow signal through intact RPE, but only in eyes with high myopia, and limited to areas of choroidal thinning. This phenomenon was previously reported by Maruko et al, who visualized choroidal blood flow in a percentage of eyes with high myopia even over areas of intact RPE utilizing this scleral projection artifact.¹³ Consistent with our observations, these patients had a thinner subfoveal choroidal thickness, likely allowing for increased signal penetration to the highly reflective sclera which enabled visualization of choroidal vessels as a projection artifact, even following scatter/absorption from the overlying RPE.

Current commercially available OCTA machines can therefore allow for visualization and study of deep choroidal vessels, though this is limited to areas of RPE atrophy. Unfortunately, current technology does not allow for flow signal to be reliably detected in normal eyes with intact RPE. This can complicate meaningful and accurate interpretation of choroidal vasculature. For example, in the absence of adjunctive imaging, the visualization of blood flow in choroidal vessels underneath a localized area of RPE atrophy could potentially be mistaken for choroidal neovascularization. To help prevent this, the practitioner must correctly identify which tissue level is being analyzed by locating the segmentation boundary lines on the B-scan OCTA image prior to interpretation.

As the largest blood supply to the eye, the choroid will undoubtedly be increasingly considered in the pathogenesis of ocular disease. Improved methods to visualize the choroid have allowed for structural characterization of the choroid across many disease states. However, given its dynamic nature, in vivo characterization of choroidal blood flow could have a major impact in elucidating the pathophysiology of chorioretinal disease. Further study is warranted to define choroidal characteristics with OCTA and future developments in OCTA technology may improve signal penetration beneath the RPE and resolve the current limitations in choroidal blood flow detection.

Acknowledgments

Funding

The author(s) disclosed receipt of the following financial support for the research, authorship, and/or publication of this article: Demetrios G. Vavvas was supported by the National Eye Institute, National Institutes of Health (grants R01 EY025362 and R21 EY023079).

References

1. Spaide RF, Fujimoto JG, Waheed NK. Image artifacts in optical coherence tomography angiography. *Retina*. 2015; 35(11):2163–2180. DOI: 10.1097/IAE.0000000000000765 [PubMed: 26428607]
2. Fixler D, Duadi H, Ankri R, Zalevsky Z. Determination of coherence length in biological tissues. *Lasers Surg Med*. 2011; 43(4):339–343. DOI: 10.1002/lsm.21047 [PubMed: 21500229]
3. Maruko I, Koizumi H, Sawaguchi S, Hasegawa T, Arakawa H, Iida T. Choroidal blood vessels in retinal pigment epithelial atrophy using optical coherence tomography angiography [published online January 13, 2017]. *Retin Cases Brief Rep*. 2017; doi: 10.1097/ICB.0000000000000542
4. Burton P, Gurrin L, Sly P. Extending the simple linear regression model to account for correlated responses: an introduction to generalized estimating equations and multi-level mixed modelling. *Stat Med*. 1998; 17(11):1261–1291. [PubMed: 9670414]
5. Huang Y, Zhang Q, Thorell MR, et al. Swept-source OCT angiography of the retinal vasculature using intensity differentiation-based optical microangiography algorithms. *Ophthalmic Surg Lasers Imaging Retina*. 2014; 45(5):382–389. DOI: 10.3928/23258160-20140909-08 [PubMed: 25230403]
6. Jia Y, Bailey ST, Hwang TS, et al. Quantitative optical coherence tomography angiography of vascular abnormalities in the living human eye. *Proc Natl Acad Sci U S A*. 2015; 112(18):E2395–E2402. DOI: 10.1073/pnas.1500185112 [PubMed: 25897021]
7. Spaide RF. Choriocapillaris flow features follow a power law distribution: implications for characterization and mechanisms of disease progression. *Am J Ophthalmol*. 2016; 170:58–67. DOI: 10.1016/j.ajo.2016.07.023 [PubMed: 27496785]
8. Mrejen S, Sarraf D, Chexal S, Wald K, Freund KB. Choroidal involvement in acute posterior multifocal placoid pigment epitheliopathy. *Ophthalmic Surg Lasers Imaging Retina*. 2016; 47(1):20–26. DOI: 10.3928/23258160-20151214-03 [PubMed: 26731205]
9. Wang JC, Lains I, Sobrin L, Miller JB. Distinguishing white dot syndromes with patterns of choroidal hypoperfusion on optical coherence tomography angiography. *Ophthalmic Surg Lasers Imaging Retina*. 2017; 48(8):638–646. [PubMed: 28810039]
10. Pellegrini M, Acquistapace A, Oldani M, et al. Dark atrophy: an optical coherence tomography angiography study. *Ophthalmology*. 2016; 123(9):1879–1886. DOI: 10.1016/j.ophtha.2016.05.041 [PubMed: 27448830]
11. Kim DY, Fingler J, Zawadzki RJ, et al. Optical imaging of the chorioretinal vasculature in the living human eye. *Proc Natl Acad Sci U S A*. 2013; 110(35):14354–14359. DOI: 10.1073/pnas.1307315110 [PubMed: 23918361]
12. Motaghianezam R, Schwartz DM, Fraser SE. In vivo human choroidal vascular pattern visualization using high-speed swept-source optical coherence tomography at 1060 nm. *Invest Ophthalmol Vis Sci*. 2012; 53(4):2337–2348. DOI: 10.1167/iovs.11-7823 [PubMed: 22410568]
13. Maruko I, Spaide RF, Koizumi H, et al. Choroidal blood flow visualization in high myopia using a projection artifact method in optical coherence tomography angiography. *Retina*. 2017; 37(3):460–465. DOI: 10.1097/IAE.0000000000001324 [PubMed: 27541926]

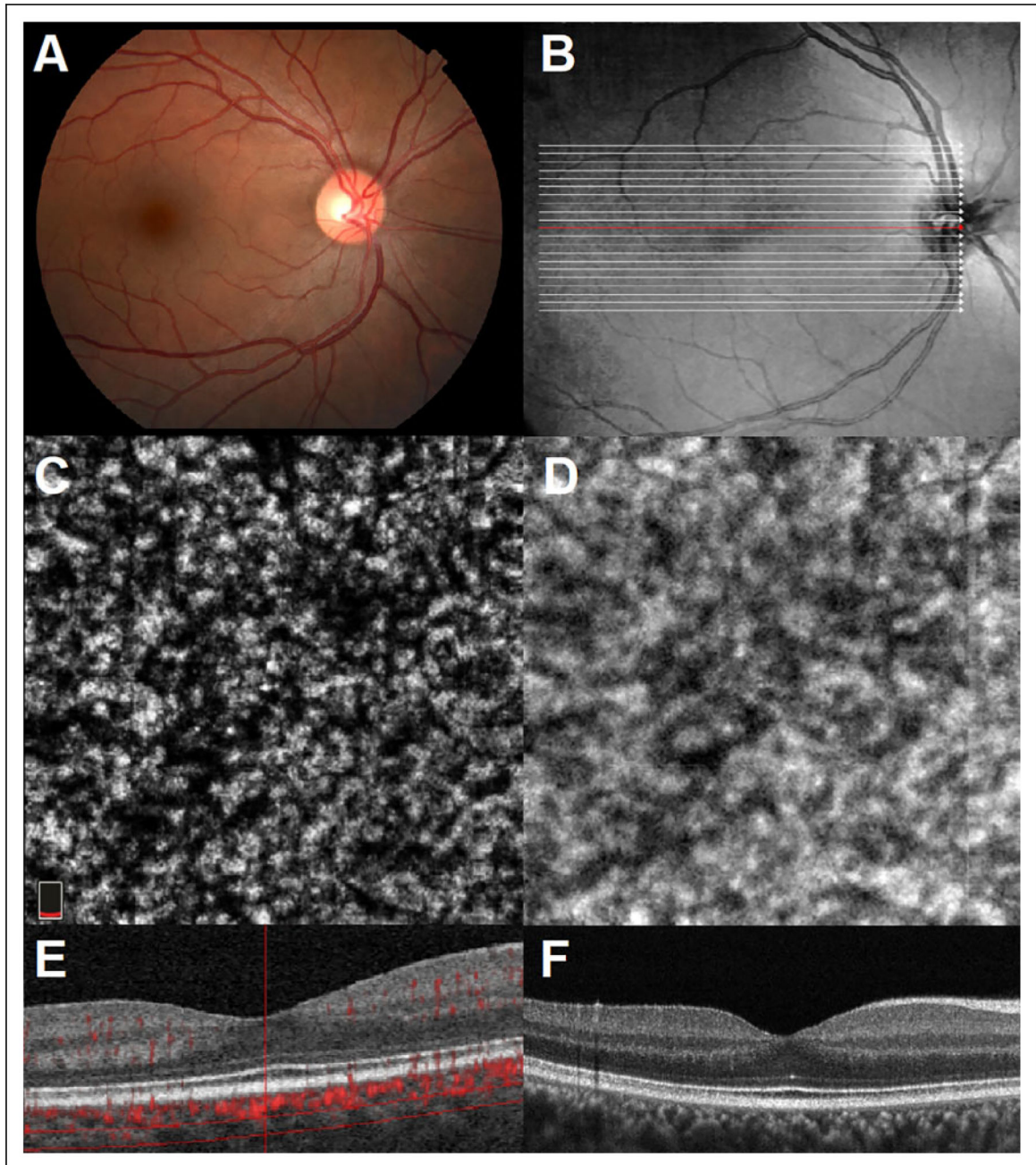


Figure 1.

(A) Color fundus photography of a normal right eye. (B) Infrared imaging with localization of B-scan acquisition through normal macula. (C) Representative 3×3 mm en face OCTA image segmented at the level of the deeper choroidal vasculature. (D) Structural en face OCT image. (E) Optical coherence tomography angiography B-scan with flow overlay and selective segmentation of the deeper choroidal vasculature (RTvue XR Avanti AngioVue). (F) Optical coherence tomography B-Scan image. OCTA indicates optical coherence tomography angiography.

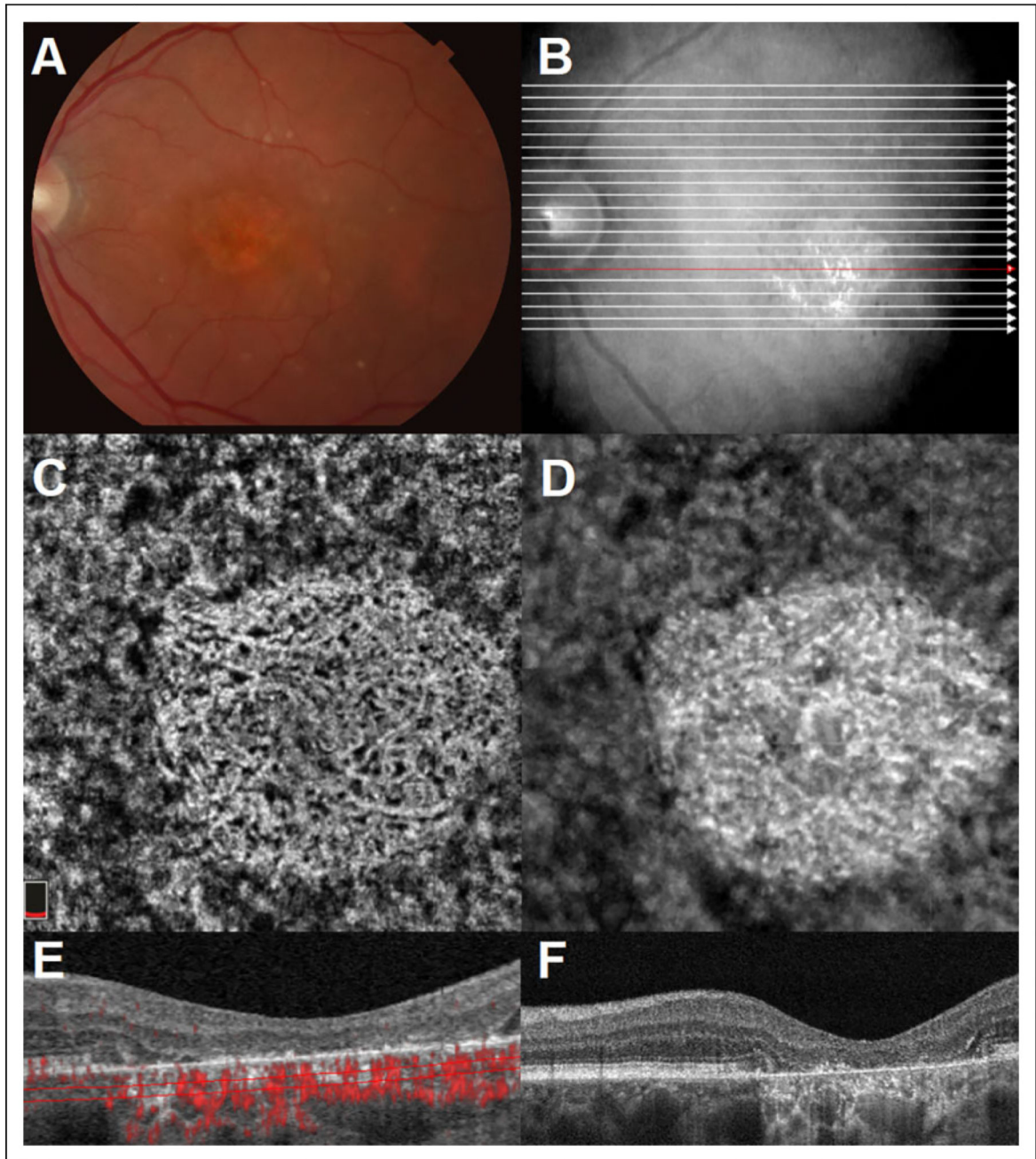


Figure 2. (A) Color fundus photography of a left eye with late stage nonexudative age-related macular degeneration. (B) Infrared imaging with localization of B-scan acquisition through affected macula. (C) Representative 3×3 mm en face OCTA image segmented through deeper choroidal vasculature and with visualization of deeper choroidal vessels. (D) Structural en face OCT image. (E) Optical coherence tomography angiography B-scan with flow overlay segmented beneath the choriocapillaris with evidence of flow within the deeper choroidal vasculature through the area of RPE atrophy (RTvue XR Avanti AngioVue). (F) Optical coherence tomography B-scan image through affected macula with hyper transmission of

signal through the area of RPE atrophy. OCTA indicates optical coherence tomography angiography; RPE, retinal pigment epithelium.

Author Manuscript

Author Manuscript

Author Manuscript

Author Manuscript

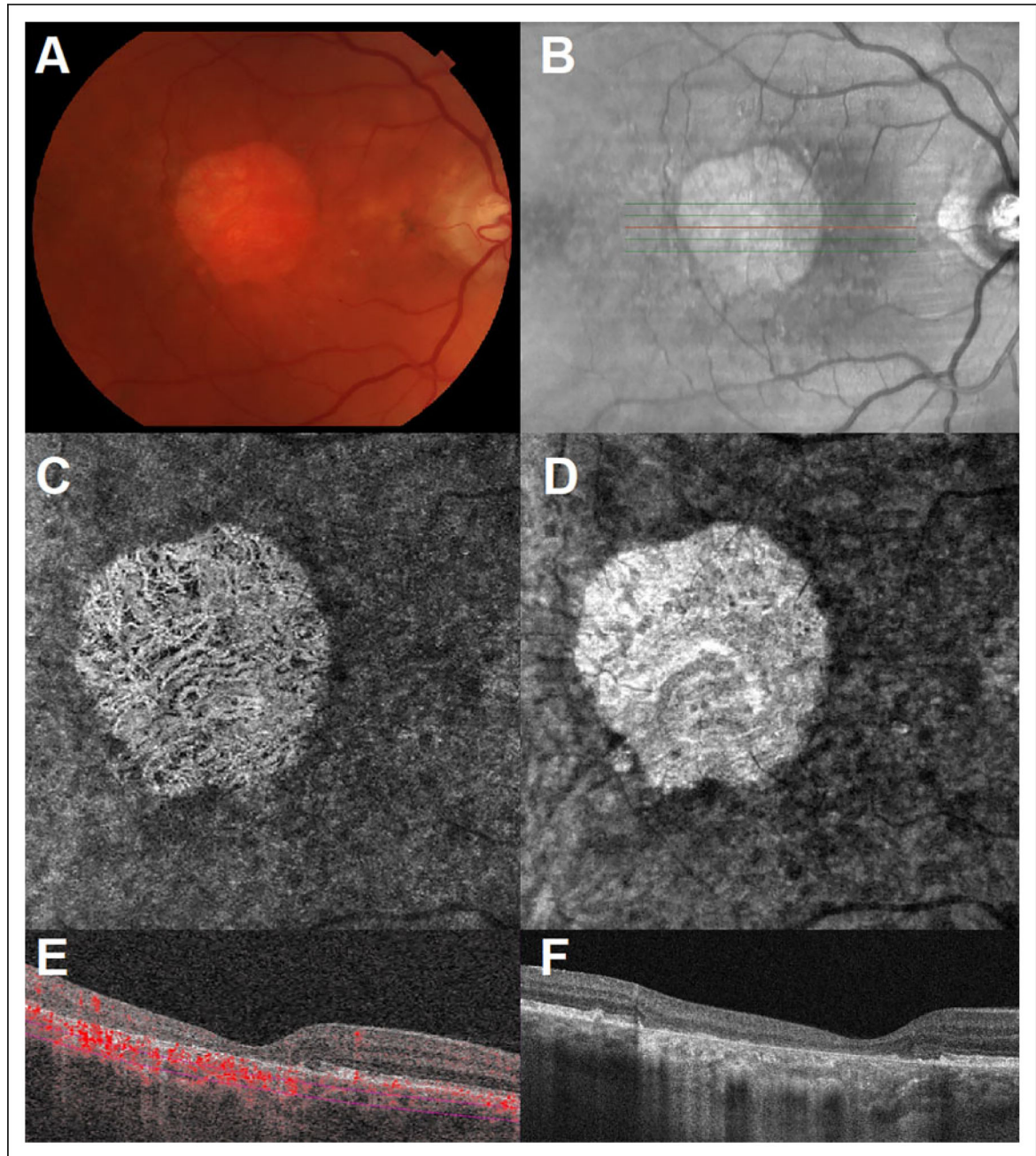


Figure 3.

(A) Color fundus photography of a right eye with late stage nonexudative age-related macular degeneration. (B) Infrared imaging with localization of B-scan acquisition through affected macula. (C) Representative 3×3 mm en face OCTA image segmented through deeper choroidal vasculature and with visualization of deeper choroidal vessels. (D) Structural en face OCT image. (E) Optical coherence tomography angiography B-scan with flow overlay and segmented beneath the choriocapillaris with evidence of flow within the deeper choroidal vasculature through the area of RPE atrophy (Cirrus HD-OCT Angioplex). (F) OCT B-scan image through affected macula with hyper transmission of signal through

the area of RPE atrophy. OCTA indicates optical coherence tomography angiography; RPE, retinal pigment epithelium.

Author Manuscript

Author Manuscript

Author Manuscript

Author Manuscript

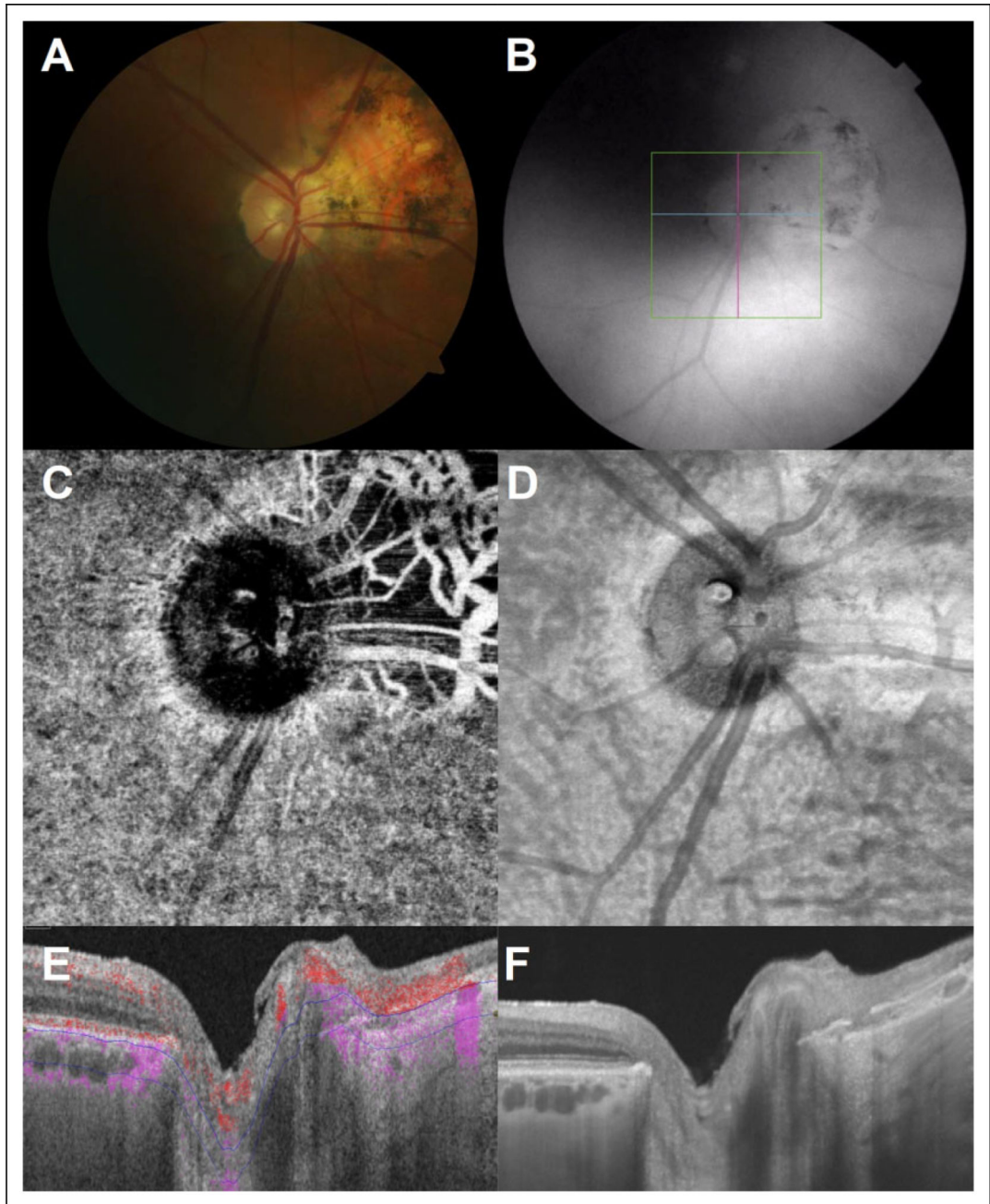


Figure 4.

(A) Color fundus photography of a right eye with an area of peripapillary atrophy nasally. (B) Infrared imaging with localization of B-scan acquisition through the optic nerve head. (C) Representative 3×3 mm en face OCTA image segmented through deeper choroidal vasculature and with visualization of the deeper choroidal vessels. (D) Structural en face OCT image. (E) Optical coherence tomography angiography B-scan with flow overlay and segmented beneath the choriocapillaris with evidence of flow within the deeper choroidal vasculature through the area of RPE atrophy nasal to the optic nerve head (DRI OCT-1 Triton). (F) Optical coherence tomography B-scan image with hyper transmission of signal

through the area of RPE atrophy. OCTA indicates optical coherence tomography angiography; RPE, retinal pigment epithelium.

Author Manuscript

Author Manuscript

Author Manuscript

Author Manuscript

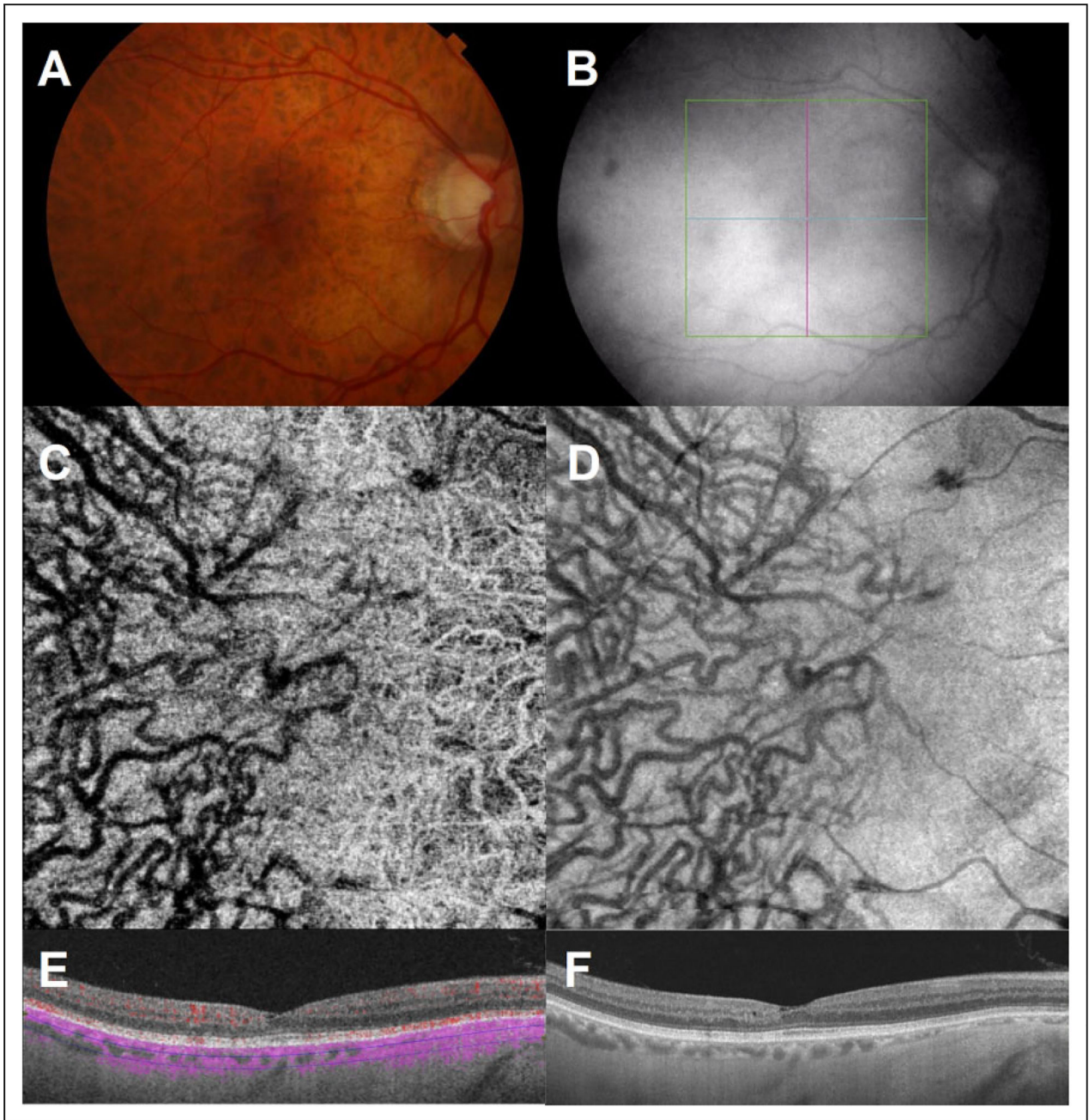


Figure 5.

(A) Color fundus photography of a right eye with high myopia. (B) Infrared imaging with localization of B-scan acquisition through the macula. (C) Representative 3×3 mm en face OCTA image. (D) Structural en face OCT image. (E) Optical coherence tomography angiography B-scan with flow overlay (DRI OCT-1 Triton). The choroid is thinner underneath the nasal macula (*50 μ m) compared to the temporal macula (*120 μ m). Segmentation is performed from 50 to 120 μ m below Bruch membrane (through choroid temporally but sclera nasally). Temporally, structural en face OCT (D) shows normal choroidal vasculature, but no choroidal flow signal is seen on OCTA (E). Nasally, choroidal

flow signal on OCTA is visualized but only when sclera is segmented (E). Corresponding structural en face OCT (D) demonstrates the absence of choroidal vasculature, suggesting that the visualization of choroidal vessels nasally within the sclera was due to a scleral projection artifact. (F) OCT B-Scan image. OCTA indicates optical coherence tomography angiography.

Author Manuscript

Author Manuscript

Author Manuscript

Author Manuscript

Table 1

Comparison of Optical Coherence Tomography Angiography Devices.

Device	Cirrus HD-OCT Angioplex	RTvue XR Avanti AngioVue	DRI OCT-1 Triton
Manufacturer	Carl Zeiss Meditec	Optovue	Topcon
OCTA algorithm	OMAG	SSADA	OCTARA
Scanning Speed	68 000 A-scans/sec	70 000 A-scans/sec	100 000 A-scans/sec
Motion correction	Real-time tracking	Real-time tracking and postscan orthogonal registration	Real-time tracking
OCTA scanning protocols	3 × 3, 6 × 6 mm centered on macula	3 × 3, 6 × 6, 8 × 8 mm centered on macula	3 × 3, 4.5 × 4.5, 6 × 6 mm centered on either macula or optic nerve head
FDA approval	Yes	Yes	No

Abbreviations: FDA, Food and Drug administration; OCTA, optical coherence tomography angiography; OCTARA, optical coherence tomography angiography ratio analysis; OMAG, optical microangiography; SSADA, split-spectrum amplitude-decorrelation angiography.

Table 2

Patient Demographics According to Imaging System.

	Cirrus HD-OCT Angioplex	RTvue XR Avanti AngioVue	DRI OCT-1 Triton
Cases, n (# of eyes)	91 (144)	77 (154)	54 (97)
Median age, years (range)	67.1 (7–93)	65 (6–91)	64.4 (24–84)
Sex, n (%)			
Female	44 (48.4)	40 (51.9)	27 (50)
Race (column %)			
Caucasian	68 (74.7)	59 (76.6)	42 (77.8)
Asian	4 (4.4)	3 (3.9)	3 (5.6)
Black	10 (11)	5 (6.5)	3 (5.6)
Hispanic	2 (2.2)	4 (5.2)	1 (1.8)
Other	3 (3.3)	3 (3.9)	1 (1.8)
Unknown	4 (4.4)	3 (3.9)	4 (7.4)

Abbreviation: OCT, optical coherence tomography.

Author Manuscript

Author Manuscript

Author Manuscript

Author Manuscript

Table 3

Summary of Diagnoses and Whether Choroidal Blood Flow Was Visualized.

Diagnosis	Cirrus HD-OCT Angioplex		RTvue XR Avanti AngioVue		DRI OCT-1 Triton	
	No. of Eyes	Eyes With + Choroid Flow Signal (%)	No. of Eyes	Eyes With + Choroid Flow Signal (%)	No. of Eyes	Eyes With + Choroid Flow Signal (%)
Nonexudative AMD	35	17 (48.6)	8	4 (50)	-	-
Exudative AMD	38	32 (84.2)	40	32 (80)	-	-
Mac Tel	4	0	12	0	21	3 (14.3)
ERM	14	0	5	0	1	0
BRVO	9	0	4	0	-	-
BRAO	-	-	4	0	-	-
CRAO	-	-	2	0	-	-
DME	12	0	10	0	-	-
NPDR	-	-	10	0	-	-
PDR	-	-	10	0	-	-
CME	-	-	5	0	-	-
WDS	2	2 (100)	-	-	4	4 (100)
PPA	-	-	-	-	17	17 (100)
Glaucoma/glaucoma suspect	-	-	-	-	34	0
CSCR	4	0	4	0	1	0
RD	3	0	2	0	2	0
Other	10	2 (20)	-	-	1	0
Normal	13	0	38	0	16	0
Total	144	53 (36.8)	154	36 (23.4)	97	24 (24.7)

Abbreviations: AMD, age-related macular degeneration; BRAO, branch retinal artery occlusion; BRVO, branch retinal vein occlusion; CME, cystoid macular edema; CRAO, central retinal artery occlusion; CSCR, central serous chorioretinopathy; DME, diabetic macular edema; ERM, epiretinal membrane; Mac Tel, macular telangiectasia; NPDR, nonproliferative diabetic retinopathy; OCT, optical coherence tomography; PPA, peripapillary atrophy; PDR, proliferative diabetic retinopathy; RD, retinal detachment; WDS, white dot syndrome.